Silicon (2020) 12:2647–2661
https://doi.org/10.1007/s12633-019-00361-9

ORIGINAL PAPER

Modification of Silica Nanoparticles with Cysteine or Methionine Amino Acids for the Removal of Uranium (VI) from Aqueous Solution

Latifa Ismail[1] · Fawwaz Khalili[1] · Faten M. Abu Orabi[1]

Received: 8 September 2019 / Accepted: 15 December 2019 / Published online: 2 January 2020

Abstract

Silica nanoparticles (SiO_2-NPs), modified silica nanoparticles with cysteine (SiO_2-Cys) or methionine (SiO_2-Meth) were used for sorption of uranium (VI) ion from aqueous solution. Silica nanoparticles and its modified forms were prepared and characterized by elemental analysis, FTIR, XRD, XRF, TGA, DSC, SEM, TEM, BET and zeta potential. Sorption of uranium(VI) ion using batch technique by silica nanoparticles, SiO_2-Cys and SiO_2-Meth was studied as a function of initial concentration, sorbent dosage, pH, contact time and temperature. The percent uptakes for silica nanoparticles, SiO_2-Cys, SiO_2-Meth were 27%, 33%, 30% respectively for U(VI) ion at 25 °C. The kinetic studies show that sorption of U(VI) ion by silica nanoparticles, SiO_2-Cys and SiO_2-Meth was well described by the pseudo second order equation. Negative values of Gibbs free energy ($\Delta G°$) suggest the spontaneity of the sorption process on silica nanoparticles and its modified forms (SiO_2-Cys) and (SiO_2-Meth). Positive values of enthalpy ($\Delta H°$) indicate endothermic adsorption process. The sorption isotherm was better fitted by Langmuir model with maximum sorption capacity for silica nanoparticles, SiO_2-Cys and SiO_2-Meth was found to be 3.6, 4.5, 3.8 mg/g respectively. Desorption studies indicate that the most favorable desorption reagent for uranium(VI) is 0.1 M HNO_3 and the highest percent recovery was achieved from silica nanoparticles (~71%) than its modified forms SiO_2-Cys and SiO_2-Meth.

Keywords Modification · Silica nanoparticles · Methionine · Cysteine · Sorption · Uranium(VI)

Abbreviations

SiO_2-NPs	Silica nanoparticles
Meth	Methionine
Cys	Cysteine
SiO_2-Cys	Modified silica nanoparticles with cysteine
SiO_2-Meth	Modified silica nanoparticles with methionine
C_o	Initial metal concentration (mg/L)
C_e	The residual concentration of the metal ion in solution at equilibrium (mg/L)
V	Volume of solution (L)
m	Mass of SiO_2-NPs, SiO_2-Cys or SiO_2-Meth (g)
K_L	Langmuir affinity constant (L/mg)
q_m	Langmuir monolayer adsorption capacity (mg/g)
q_e	The equilibrium amount of metal ion adsorbed per unit mass of adsorbent (mg/g)
q_t	The amount of metal ions adsorbed (mg/g) at contact time t
k_2	The second order reaction constant (g/mg.min)

✉ Latifa Ismail
latifa.saeed@yahoo.com

Fawwaz Khalili
fkhalili@ju.edu.jo

Faten M. Abu Orabi
fatenaladwan_i@yahoo.com

[1] Chemistry Department, The University of Jordan, 11942, Amman 9626535000, Jordan

1 Introduction

Pollution with uranium(VI) has been studied for human health and animals. Uranium is the most important natural radioactive elements effecting the environment and caused renal damage then kidney failure and death; therefore removal of uranium from aqueous solution is very important [1, 2]. A variety of techniques have been applied for removal of U(VI) from aqueous solutions such as, evaporation, ion exchange, solvent

extraction, transport through membranes and precipitation are unsuccessful for the removal of trace amount of pollutants [3]. Adsorption is efficient and convenient for removal of radioactive elements due to its low cost, high capacity and ease of regeneration. Natural and synthetic adsorbents such as perlite [4], organoclay [5], alumina [6], activated carbons [7], bentonite [8], zeolite [9], nanoporous [10] and biological materials [11] have been tested for sorption of uranyl ion from aqueous solution.

Mesoporous nanosilica is considered as promising adsorbent due to its high surface area, tunable and uniform pore structure, high pore volume, ordered pore structure, thermal and mechanical stability and extraordinarily wide possibilities for functionalization. Nanosilica is used in several scientific and industrial applications [12], controlling the release of medicines and as biosensors [13]. The silica surface is composed of siloxane bridges (-Si-O-Si-) and silanol groups (Si-OH). The silica surface becomes negatively charged when pH of the solution is larger than two where the silanol groups tend to be deprotonated as $Si\text{-}O^-$ [14]. At pH greater than its isoelectric point (>2), silica exhibits ion exchange capabilities via the weakly acidic silanol groups and can be used to adsorb various types of inorganic and organic contaminant in water.

Cysteine and methionine are amino acids containing sulfur atom. Cysteine is a hydrophilic amino acid due to the presence of thiol group, whereas methionine has a hydrophobic and nonpolar aliphatic side chain [15]. Thiol group in cysteine molecule has many biological functions [16]. Amino acids may exist either as uncharged molecule ($H_2N\text{-}CHR\text{-}COOH$) or as zwitterions ($^+H_3N\text{-}CHR\text{-}COO^-$) depending on the pH of solution and the isoelectric point [17]. Due to silica excellent stability and great abundance on earth, several applications have been found for the pure and the modified with amino acids or others.

The interactions between biochemical molecules and inorganic materials have a significant impact on bionanotechnology [18], drug delivery research [19], bionanocomposite materials and biomedical applications [20]. Numerous researches have investigated the sorption of amino acids by various materials including polymeric adsorbent [21], mineral [22], activated carbon [23] and zeolite [24]. Recently, several researchers targeted the sorption of amino acids by mesoporous silica-based. The suggested mechanisms for sorption are electrostatic interactions, hydrogen bond formation, ion exchange and ligand-exchange through carboxyl and amino groups [25].

Particles in nano sized scale tend to agglomerate because of the high surface energy and abundant hydroxyl groups on the silica surface, so a modification to produce a hydrophobic surface is necessary to improve the dispersion and compatibility of silica nanoparticles (SiO_2-NPs) [26].

The aim of this study is to modify Aldrich silica nanoparticles with cysteine or methionine amino acids in order to decrease the agglomeration of silica nanoparticles and to increase functional groups on the silica surface which enhance the uptake of U(VI) ions from aqueous solution. Sorption of U(VI) ions onto silica nanoparticles and its modified forms were done at different time, pH, temperature, and metal ion concentration using batch technique. Different models have been used to study the sorption isotherm data such as; Langmuir, Freundlich, and Dubinin-Radushkevich (D-R). The kinetic and thermodynamic parameters of sorption have been calculated then desorption after sorption was studied.

2 Materials and Methods

2.1 Chemicals

All reagents used in this study were of analytical grade reagents. Silicon dioxide nanopowder, 10–20 nm particle size (BET), 99.5% trace metals basis, L-Methionine reagent grade ≥ 98% (HPLC) and L-Cysteine 98% cell culture tested from Sigma Aldrich. Hydrochloric acid (HCl) 37%, nitric acid (HNO_3) 69% and glacial acetic acid from Tedia, sodium hydroxide pellets (NaOH) from SDS vorte partenaire chimie, sodium perchlorate ($NaClO_4$) from Acros, cadmium chloride monohydrat ($CdCl_2.\ H_2O$) from Merck, ninhydrin from Riedel de Haen, uranyl(VI) nitrate hexahydrate ($UO_2(NO_3)_2.\ 6H_2O$) from BDH chemicals Ltd. Poole, England. Arsenazo (III) indicator from Janseen chimica while absolute ethanol (99.5%) and acetone from Selvo chem.

2.2 Instruments

Weighing was done using RADWAG ® AS 220. R2, Electronic Balance. Filtration was done using Syringe Filters Nylon 0.4 μm. The pH of solution was measured using EUTECH pH–meter. Fourier-transform infrared spectroscopy (FT-IR) spectra were done using Thermo Nicolet NEXUS 670 FTIR spectrophotometer with KBr disc. Centrifugation was done using (DJB Lab Care-AIC PK 130) at 2500 RPM speed. Elemental analyses were obtained with a Euro EA3000 CHNS-O elemental analyzer (Milan, Italy). Thermal Gravimetric Analysis (TGA) were carried using NETZCH STA 409 PG/PC Thermal Analyzer in the temperature range (0–800 °C) at a heating rate of 20 °C/min. Thermal stability and melting was carried by NETZCH Differential Scanning Calorimeter (DSC) 204 F1 in the temperature range (0–800 °C) at a heating rate of 10 °C/min. X-Ray Diffraction (XRD) was measured using Philips X pert PW 3060, operated at 45 kV and 40 mA. The chemical composition of the samples was determined by X-ray fluorescence (Shimadzu XRF-1800). The shape with three dimensional (3D) and surface morphology was examined with NCFL's FEI QUANTA 600 FEG scanning electron microscope (SEM). Samples were

shaken using GFL-85 thermostatic shaker. The concentration of the U(VI) ion was determined using Vis-spectrophotometer from METASH model V-5100, and a 1.0 cm quartz cell. BET (Brunauer-Emmett-Teller) method was used to measure specific surface area (SSA) of the powder from sorption desorption of N_2 at 77.3 K with Nova 220e surface area and pore size analyzer. Zeta potential was carried using Microtrac particle size analyzer.

2.3 Modification of Silica Nanoparticles with Cysteine or Methionine

A 60.0 g of the silica nanoparticles (SiO_2-NPs) was mixed with 60.0 g ± 0.1 mg of cysteine in 600.0 mL deionized water for 48 h. On the other hand, a 60.0 g of the silica nanoparticles was mixed with 24.0 g ± 0.1 mg of methionine in 1 Liter deionized water for 48 h. Then the mixture in both cases SiO_2-Meth or SiO_2-Cyst was centrifuged, washed with deionized water several times and the solid was dried in vacuum oven at 25 °C to a constant weight. The amount of cysteine or methionine remaining in the filtrate solution was determined by Vis-spectrophotometer using Cd-ninhydrine solution after constructing up an analytical calibration curve [27].

2.4 Sorption Experiments

Kinetic studies were used to determine the equilibrium time for sorption of U(VI) by silica nanoparticles (SiO_2-NPs) and its modified forms using batch technique. Shaking 0.1 g ± 0.1 mg of the silica nanoparticles and its modified forms in 100 mL plastic bottle with 25.0 mL of 50 mg/L U(VI) ion solution at pH 3.0, the contact time varied from 15 to 1440 min at 25.0, 35.0 and 45.0 °C. The mixture was filtered with nylon micro filter 0.45 μm and the amount of U(VI) ion remaining in the filtrate solution was determined by Vis-spectrophotometer using Arsenazo(III) indicator [28].

2.5 Rate of Metal Ion Uptake

The percent uptake of U(VI) ion from aqueous solution and the sorption capacity (qe) have been calculated using the following equations:

$$\%\text{uptake} = (C_o - C_e)/C_o \times 100\% \quad (1)$$

$$q_e = (C_o - C_e)V/m \quad (2)$$

Where C_o is the initial U(VI) concentration (mg/L), C_e the remaining concentration of U(VI) in solution at equilibrium, V the volume of U(VI) solution (L) and m the mass of the silica nanoparticles (SiO_2-NPs) or its modified forms (g).

2.6 Sorption Kinetic

In order to clear the adsorption mechanism of U(VI) onto silica nanoparticles and its modified forms, kinetic investigations were tested using the following models.

Pseudo-first-order

$$\ln(q_e - q_t) = \ln q_e - k_1 t \quad (3)$$

Pseudo-second-order

$$t/q_t = 1/k_2 q_e^2 + t/q_e \quad (4)$$

Where, q_e and q_t (mg/g) are the amount of U(VI) adsorbed onto silica nanoparticles (SiO_2-NPs) and its modified forms at equilibrium and time t (min) respectively. k_1 (min^{-1}) is the rate constant for the pseudo-first-order and k_2 is the rate constant for the pseudo second-order (g/mg.min) adsorption process [29].

2.7 Adsorption Isotherms

Three types of isotherm models were used to study the sorption of U(VI) onto silica nanoparticles and its modified forms: Langmuir [30], Freundlich [31] and Dubinin–Radushkevich [32]. The sorption isotherms of U(VI) onto silica nanoparticles and its modified forms were carried out by shaking 0.1 g silica nanoparticles or its modified forms with 25.0 mL of metal ion solution of different concentrations ranging from 10 to 50 mg/L at pH 3 for one hour and at different temperatures (25.0, 35.0 and 45.0 °C).

The following formulas are used to study the adsorption isotherms:

- Langmuir equation (Form II)

$$1/q_e = (1/(q_m K_L))\ 1/C_e + 1/q_m \quad (5)$$

- Freundlich equation

$$\text{Log } q_e = \log K_F + 1/n \log C_e \quad (6)$$

- Dubinin-Radushkevich equations

$$\ln q_e = \ln q_{max} - \beta \varepsilon^2 \quad (7)$$

Table 1 Elemental analysis results for silica nanoparticles and its modified forms

Sample	%C	%H	%N
SiO_2-NPs	1.9	1.6	–
SiO_2-Cys	12.8	2.6	4.2
SiO_2-Meth	4.4	1.8	0.7

The Polanyi potential ε, equals to:

$$\varepsilon = RT\ In\ (1 + 1/C_e) \quad (8)$$

2.8 Desorption Experiments

Desorption of the U(VI) ion was carried under batch experiment. By loading 0.5 g silica nanoparticles or its modified forms; (SiO_2-Cys) and (SiO_2-Met) with 25.0 mL of 50 ppm of U(VI) solution in 50.0 mL centrifuge tube and shaking for 24 h, then centrifuged, decanted and washed the remaining solid with deionized water several times. In the same centrifuge tube, desorption was tested using 25.0 mL of two eluting agents, 1.0 M HNO_3 and 0.1 M HNO_3 on two different samples of silica nanoparticles and its modified forms (SiO_2-Cys) and (SiO_2-Met) to recover adsorbed metal ions. Desorption procedure was repeated three times to completely remove metal ions. The concentration of metal ion in the collected three elutes was determined by Vis-spectrophotometer to calculate percentage removal of U(VI) ion.

3 Results and Discussion

3.1 Characterization of Silica Nanoparticles and its Modified Forms

The silica nanoparticles and its modified forms; (SiO_2-Cys) and (SiO_2-Meth) were characterized by elemental analysis, Fourier-transform infrared spectroscopy (FTIR), X-ray fluorescence (XRF), X-ray diffraction (XRD), scanning electron microscope (SEM), transmission electron microscope (TEM), N_2-sorption/desorption isotherm (BET), zeta potential (ζ), thermogravimetric analysis (TGA) and differential scanning calorimetry (DSC).

3.1.1 Elemental Analysis

Increasing the percentage of carbon, hydrogen and nitrogen in modified silica nanoparticles comparing with unmodified forms indicated a successful surface functionalization of silica nanoparticles with cysteine or methionine and this result

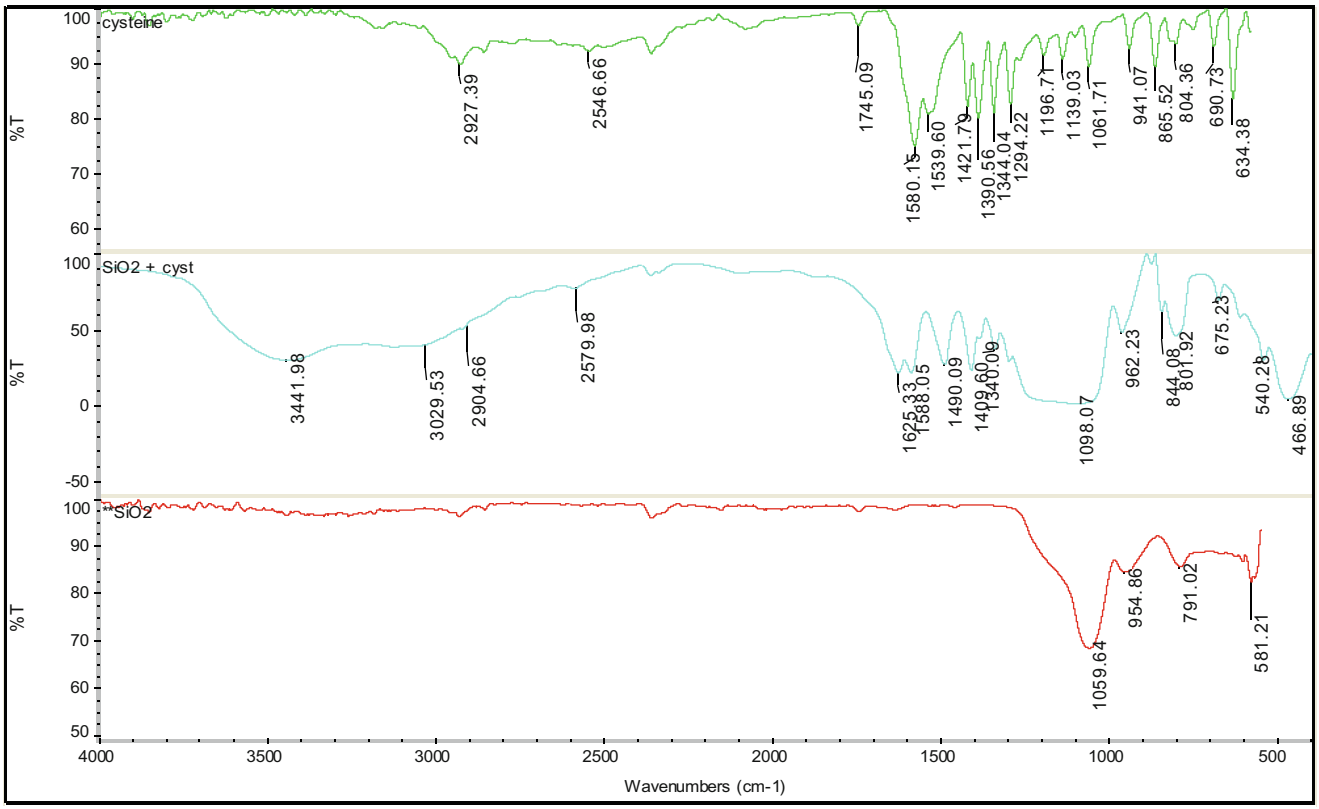

Fig. 1 FTIR spectra for the silica nanoparticles, SiO_2-Cys and cysteine

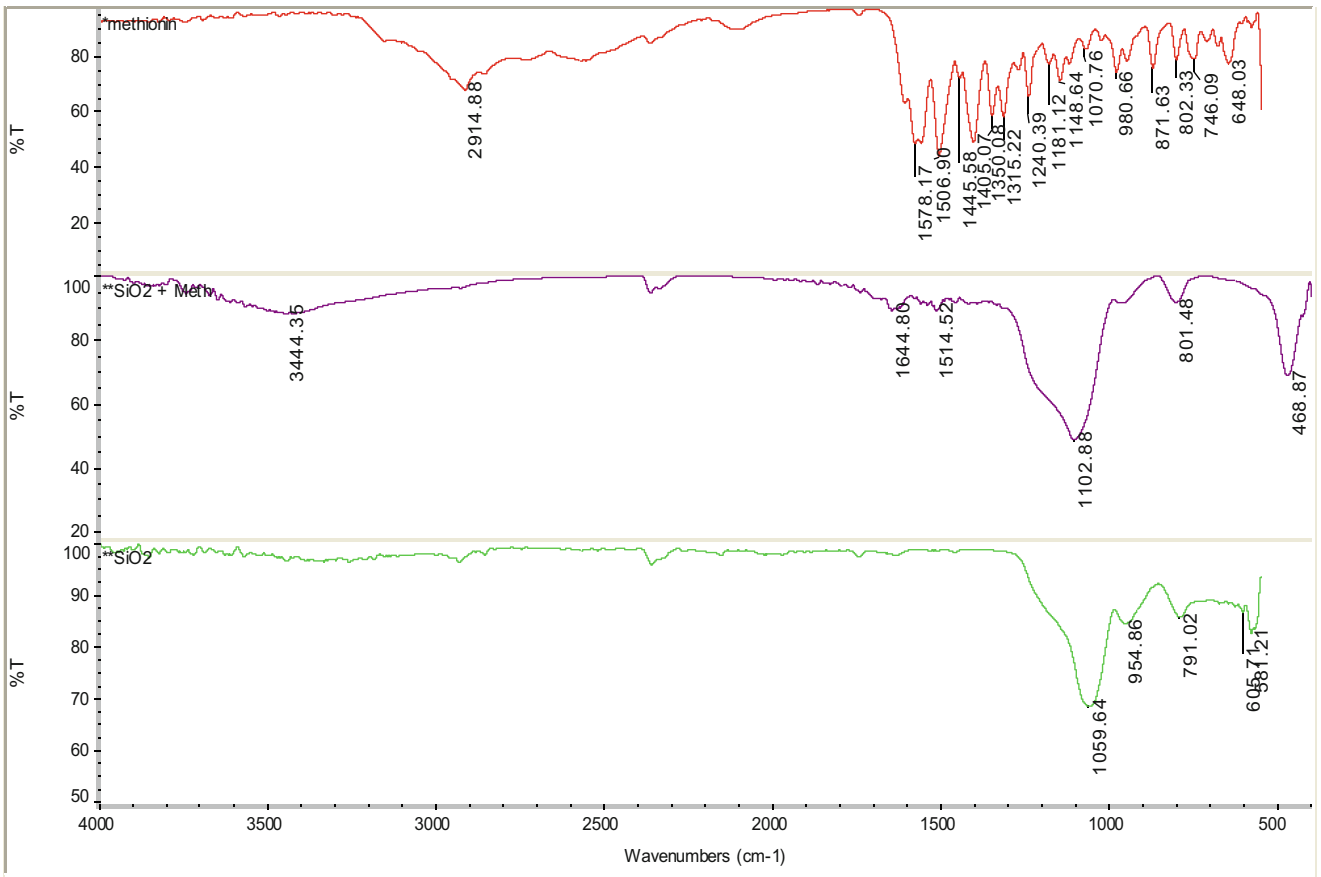

Fig. 2 FTIR spectra for the silica nanoparticles, SiO_2-Meth and methionine

agrees with the following FTIR, XRD and XRF results (Table 1).

3.1.2 Fourier-Transform Infrared Spectroscopy (FTIR)

The FTIR spectra of silica nanoparticles (SiO_2-NPs), cysteine and modified silica nanoparticles with cysteine (SiO_2-Cys) are shown in Fig. 1, whereas the FTIR spectra of silica nanoparticles (SiO_2-NPs), methionine and modified silica nanoparticles with methionine (SiO_2-Meth) are shown in Fig. 2. All the characteristic bands are listed in Table 2.

The FTIR analysis was performed in order to establish the changes in the functional groups of the silica nanoparticles and its modified forms (Figs. 1 and 2). The FTIR

Table 2 Characteristic FTIR bands for silica nanoparticles and its modified forms

Assignment	SiO_2-NPs Band (cm^{-1})	SiO_2-Cys Band (cm^{-1})	SiO_2-Meth Band (cm^{-1})	Methionine Band (cm^{-1})	Cysteine Band (cm^{-1})
Si–O–Si asymmetric	1059	1098	1102	–	–
Si–O–Si symmetric	791	801	801	–	–
Si–O–Si bending	581	466	468	–	–
Si-OH stretching	955	962	960	–	–
$–NH_3^+$ asymmetric.	–	3442	3444	–	–
$–CH_2$ asymmetric.	–	2904	w.b*	2915	2927
$–NH_3^+$ bending	–	1588	1514	1507	1539
$–COO^-$asymmetric.	–	1625	1645	1578	1580
$–COO^-$ symmetric	–	1490	w.b*	1446	1422
–S–H stretching	–	2580	–	–	2546
$–S–CH_3$ stretching	–	–	1316	1315	–

*w.b: weak band

Table 3 Chemical composition (weight %), of silica nanoparticles and its modified forms

Chemical composition	SiO_2-NPs (weight %)	SiO_2-Cys (weight %)	SiO_2-Meth (weight %)
Si	98.8	82.0	86.8
S	1.2	17.9	13.1

spectrum of silica nanoparticles showed characteristic peaks at 1059, 791 and 581 cm^{-1} which were related to the asymmetric, symmetric, and bending modes of Si–O–Si, respectively and 955 cm^{-1} for Si-OH stretching vibration of the silanol group [33]. The FTIR spectrum for the modified silica nanoparticles with cysteine (Fig. 1) showed additional broad peak at 3440 cm^{-1}, corresponding to the ammonium asymmetric stretching band. Also additional peaks appearing at 1600, 1500 and 1400 cm^{-1} were related to COO^- asymmetric stretching, N-H bending and COO^- symmetric stretching respectively [34]. The presence of carboxylate and ammonium peaks indicate that cysteine molecule exist in zwitterion form. Also a weak band at 2580 cm^{-1} is attributed to the S-H stretching in cysteine, the presence of this band indicated that sulfur atom is not bound to silanol groups. Other authors observed the vanishing of the S-H stretching band when they studied the interaction of cysteine with different minerals, which contributed to bonded sulfur atom with the mineral surface [35]. The FTIR spectrum for the modified silica nanoparticles with methionine (Fig. 2) showed also additional broad peak at 3444 cm^{-1} corresponding to the ammonium asymmetric stretching band. Additional peaks appearing at 1645, 1514 and 1316 cm^{-1} were related to COO^- asymmetric stretching, N-H bending stretching and S-C stretching bands, respectively [36]. The differences in the spectra for silica nanoparticles and modified silica nanoparticles with cysteine or methionine indicated that the amino acids were successfully attached to silanol group or silica surface through the ammonium group.

3.1.3 X-Ray Fluorescence (XRF)

X-ray fluorescence (XRF) was used to determine the metallic ion composition of the silica nanoparticles and its modified forms; (SiO_2-Cys) and (SiO_2-Meth). The results presented in Table 3 showed the high content of sulfur in the modified silica nanoparticles with cysteine or methionine which indicated the association of cysteine or methionine with silica nanoparticles.

3.1.4 X-Ray Diffraction (XRD)

Figure 3 represents the X-ray diffraction pattern of the silica nanoparticles and its modified forms; (SiO_2-Cys) and (SiO_2-Meth). The silica nanoparticles (SiO_2-NPs) and its modified forms patterns showed a broad peak at $2\theta = 22.50°$, which is a known characteristic peak for amorphous silica [37]. The modified silica nanoparticles with cysteine (SiO_2-Cys) pattern showed the presence of two sharp peaks at $2\theta = 18.95°$ and $2\theta = 33.16°$ related to monoclinic crystalline cysteine [38]. While, the modified silica nanoparticles with methionine (SiO_2-Meth) pattern showed the presence of two sharp peaks at $2\theta = 5.16°$ and $2\theta = 23.21°$ related to monoclinic crystalline methionine [39]. The presence of sharp peaks in X-ray diffraction pattern of the modified silica nanoparticles, ensure the existence of crystalline amino acid with silica nanoparticles.

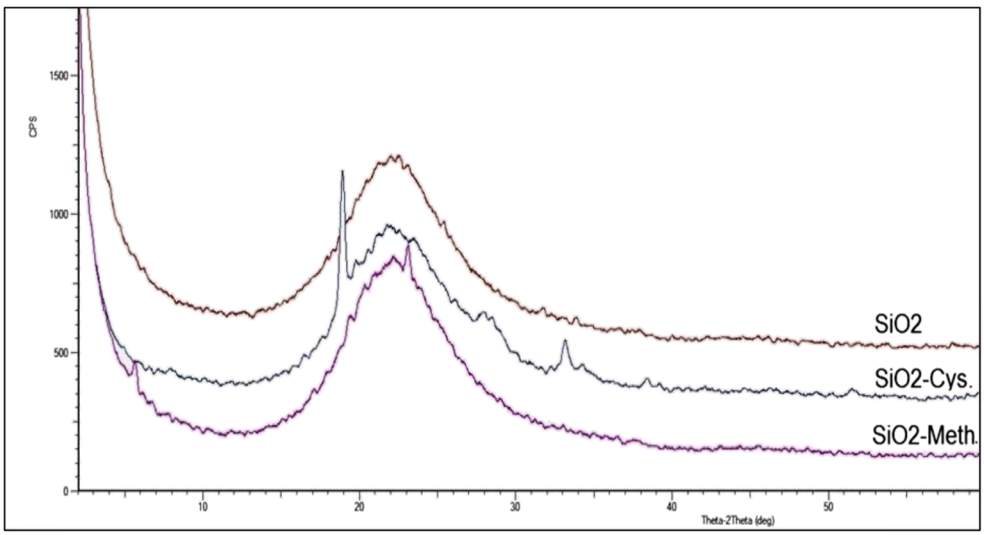

Fig. 3 X-ray diffraction pattern of silica nanoparticles and its modified forms

3.1.5 Scanning Electron Microscope (SEM)

The morphology for silica nanoparticles (SiO_2-NPs) and its modified forms were investigated using scanning electron microscope (SEM). All SEM images (Fig. 4) indicated that the particles are agglomerate, various sizes, irregular morphology, and particles size more than 1 μm [40] with no marked effect of cysteine or methionine.

3.1.6 Transmission Electron Microscope (TEM)

Transmission electron microscope (TEM) was used to investigate the morphology information of silica nanoparticles (SiO_2-NPs) and its modified forms; (SiO_2-Cys) and (SiO_2-Meth) such as particle size and particle shape. TEM micrographs of silica nanoparticles and its modified forms were presented in Fig. 5, which clearly showed the spherical like morphology of silica nanoparticles and its modified forms with average particle size of 10–20 nm [41]. Figure 5a showed particle size about 23 nm for silica nanoparticles, whereas Fig. 5b showed particle size about 16 nm for SiO_2-Cys and finally Fig. 5c showed particle size about 14 nm for SiO_2-Meth.

TEM micrographs showed that the particle size of modified silica nanoparticles is smaller than silica nanoparticles, which is related to sample preparation with sonication. This result agrees with zeta potential results; the high value of negative charge on the surface of modified silica nanoparticles with cysteine or methionine increases the repulsion between particles which lead to decrease the agglomeration of particles and decrease particle size [42].

3.1.7 Nitrogen Sorption/Desorption Isotherm (BET)

Brunauer-Emmett-Teller (BET) equation has been used to calculate the specific surface area (m^2/g) and the average pore diameter (nm) for silica nanoparticles (SiO_2-NPs) and its modified forms; (SiO_2-Cys) and (SiO_2-Meth). Table 4 summarized the nitrogen sorption/desorption isotherms results. The silica nanoparticles (SiO_2-NPs) exhibited type IV sorption isotherm with an H1 hysteresis type as shown in Fig. 6 [43].

The modified silica nanoparticles with cysteine (SiO_2-Cys) have the lowest specific surface area (92.0 m^2/g) than modified silica nanoparticles with methionine (121.5 m^2/g) and silica nanoparticles (139.9 m^2/g). This refer to coverage of silica nanoparticles surface with amino acids, which decrease the available surface area of silica nanoparticles. The lowering in surface area ensures the modification of silica nanoparticles and related to the percentage loading of cysteine on silica nanoparticles

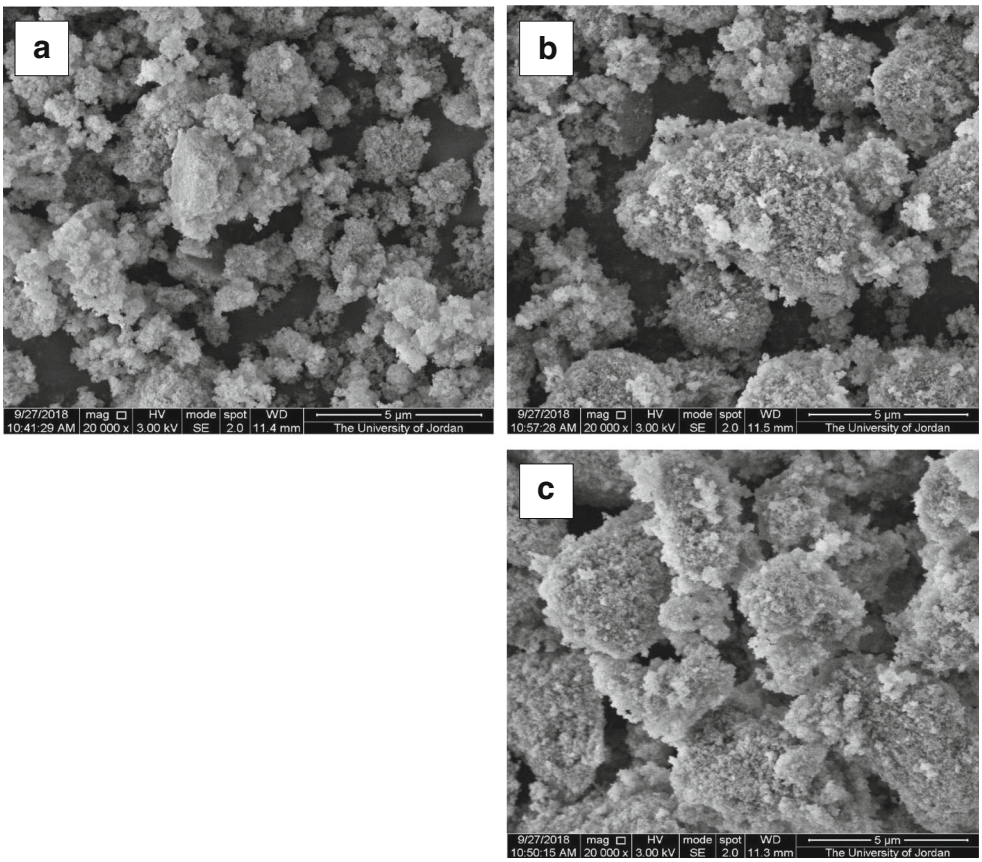

Fig. 4 SEM micrographs of **a** silica nanoparticles, **b** SiO_2-Cys, (c) SiO_2-Meth

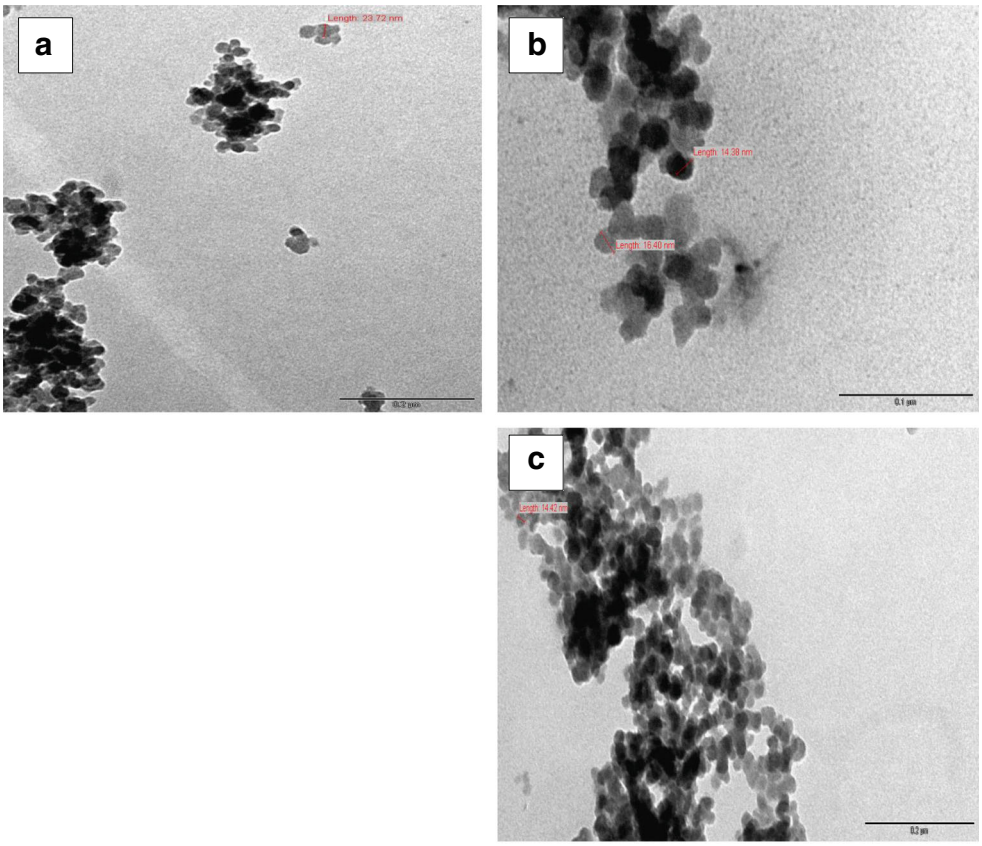

Fig. 5 TEM micrograph of **a** silica nanoparticles, **b** SiO_2-Cys, **c** SiO_2-Meth

surface, which is more than the percentage loading of methionine [44, 45]. The average pore diameter for silica nanoparticles is 10.0 nm, which classified it as mesoporous silica [43], whereas the average pore diameter for SiO_2-Cys and SiO_2-Meth is 7.7 and 7.6 nm respectively. The small decrease in average pore diameter with the addition of cysteine or methionine results from the occupation of pore space by the amino acids.

3.1.8 Zeta Potential

Table 4 shows that ζ potential of unmodified silica nanoparticles and its modified forms having negative values in water at pH 3.0, which indicates negative surface charge. The large negative value of unmodified silica nanoparticles (−69.2 mV) indicated a highly stable dispersion silica nanoparticles [42]. However, the ζ potential of modified silica nanoparticles with cysteine (−69.7 mV) and with methionine (−71.9 mV) showed to be more negative than unmodified silica nanoparticles. These prove the presence of amino acids in zwitterion forms and ammonium group interact with silanol groups while the carboxylate is free [46]. Zeta potential results indicated the high dispersion of the two modified in comparison with the unmodified silica nanoparticles [47], and confirm a successful surface functionalization of silica nanoparticles (SiO_2-NPs) with cysteine or methionine amino acids.

Table 4 Main characteristics of silica nanoparticles and its modified forms

Sample	ζ (mV)	S_{BET} (m^2/g)	Average pore diameter(nm)
SiO_2-NPs	−69.2	139.9	10.0
SiO_2-Cys	−69.7	92.0	7.7
SiO_2-Meth	−71.9	121.5	7.6

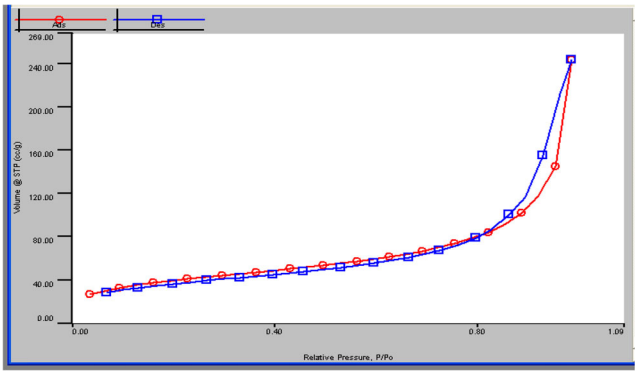

Fig. 6 Nitrogen sorption/desorption isotherm for silica nanoparticles

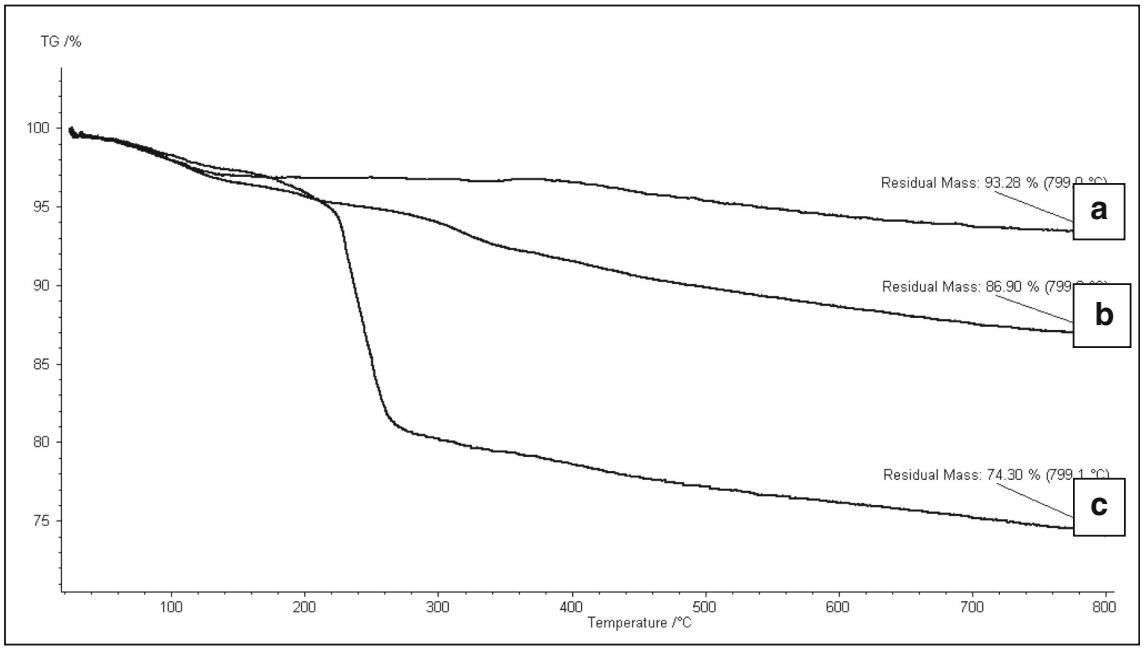

Fig. 7 TGA thermogram of **a** silica nanoparticles, **b** SiO_2-Meth, **c** SiO_2-Cys

3.1.9 Thermal Properties

Thermogravimetric Analysis (TGA) Figure 7 shows the TGA thermogram of silica nanoparticles (SiO_2-Nps) and its modified forms with cysteine or methionine. The TGA thermogram for silica nanoparticles (Fig. 7a) showed a weight loss (about 6 wt%) after 100 °C, which is related to the elimination of physically adsorbed water on the surface [48]. The TGA thermogram for modified silica nanoparticles with methionine (Fig. 7b) showed two weight loss stages. The first weight loss stage before 200 °C, can be related to the physically adsorbed water and the second small weight loss (about 13 wt%) stage at 300 °C may be attributed to the decomposition of methionine. Also, the TGA thermogram for modified silica with cysteine (Fig. 7c) showed two weight loss stages. The first weight loss occurred before 200 °C, which is similar to that

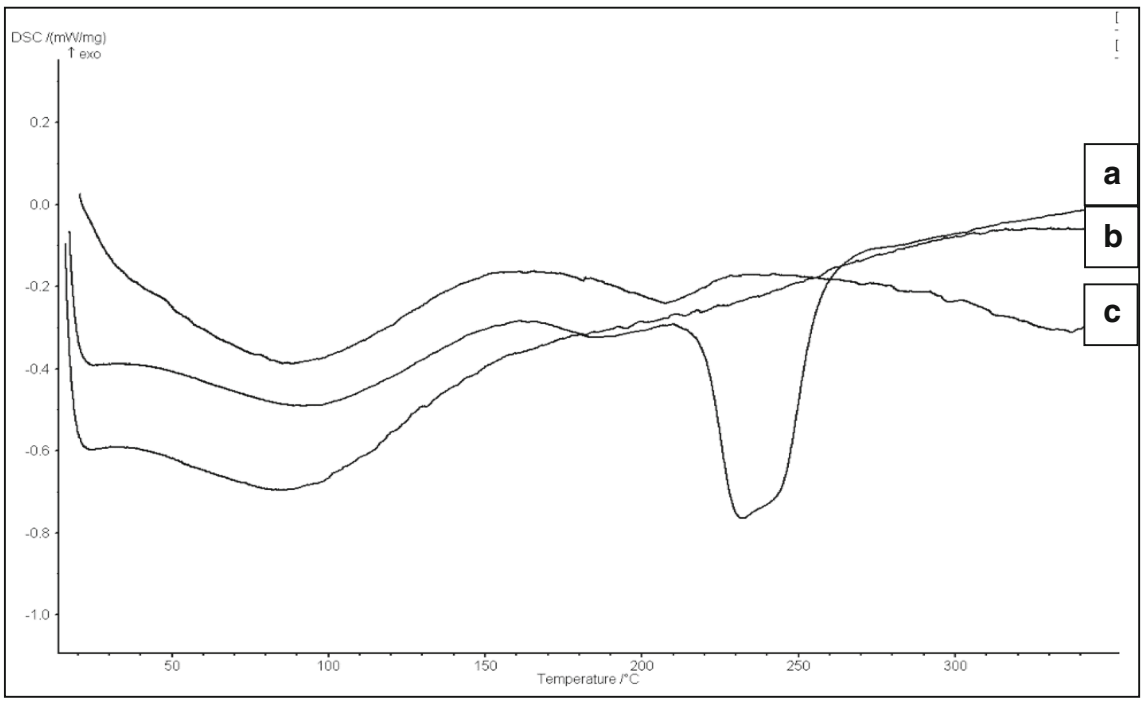

Fig. 8 DSC thermograms of **a** silica nanoparticles, **b** SiO_2-Cys, **c** SiO_2-Meth

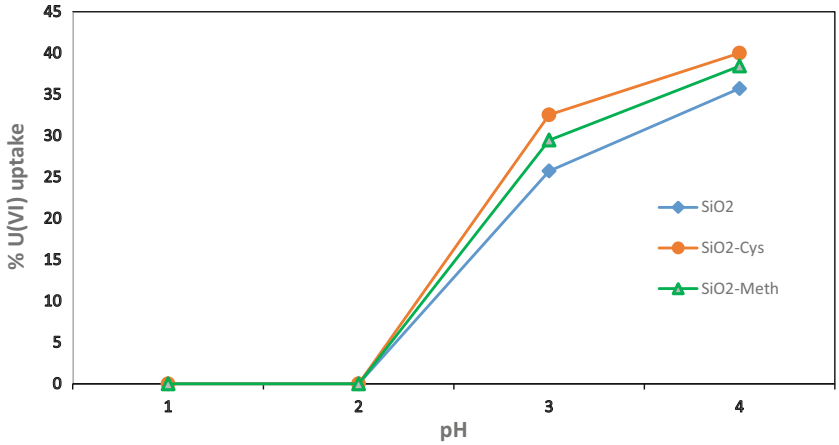

Fig. 9 Percent uptake of U(VI) by unmodified and modified silica nanoparticles at different pH, 25 °C, 24 h and 0.1 g adsorbent

of SiO_2-Meth, whereas the second sharp weight loss (about 26 wt%) at 230 °C attributed to the decomposition of cysteine [49]. The percentage of weight loss of SiO_2-Cys is more than percentage of weight loss of SiO_2-Meth, which is due to the higher percentage loading of cysteine than methionine by silica nanoparticles [50].

Differential Scanning Calorimetry (DSC) To evaluate the degree of purity of a compound the differential scanning calorimetry (DSC) method has been satisfactorily used [39]. Figure 8a showed glass transition temperature at 90 °C for silica nanoparticles and its modified forms; (SiO_2-Cys) and (SiO_2-Meth), which is a result of the presence of the amorphous silica nanoparticles. Whereas, Fig. 8b showed the DSC thermogram analysis for modified silica nanoparticles with cysteine (SiO_2-Cys). The presence of melting transition temperature at 230 °C as broad peak indicated that cysteine is not pure and it is associated with silica nanoparticles surface [49]. Also, Fig. 8c showed the DSC thermogram analysis for SiO_2-Meth. The melting transition temperature showed as weak peak at 205 °C due to the low percentage loading of methionine on surface of silica nanoparticles and this agrees with thermogravimetric analysis results.

3.2 Effect of pH

According to literature [51], uranyl ions would be precipitated in the form of $UO_2(OH)_2$ at pH value higher than 5.0 if uranyl ions concentration exceeded 1.0 mmol L^{-1}. Sorption behavior of U(VI) by unmodified and modified silica nanoparticles has been studied by changing the pH values of aqueous solution from pH 1.0 to 4.0. It can be clearly seen from Fig. 9 that the percentage uptake of U(VI) by unmodified and modified silica nanoparticles were zero at pH 1.0~2.0, which insure the presence of competitive sorption on the surface of unmodified and modified silica nanoparticles between H_3O^+ and U(VI) at low pH, and the existence of repulsive force between the protonated surface and positive metal ions limited the approach of U(VI). Raising the pH of solution from 3.0 to 4.0 will increase the percentage uptake of U(VI) on silica nanoparticles (SiO_2-NPs) and its modified forms. Decreasing the concentration of H^+ could decrease the positive charges or increase the negative charges on silica nanoparticles surface so the U(VI) ions will be adsorbed on the silica nanoparticles surface. The adsorption of U(VI) by silica nanoparticles (SiO_2-NPs) and its modified forms was done at pH 3.0 to prevent hydrolysis of uranyl ion.

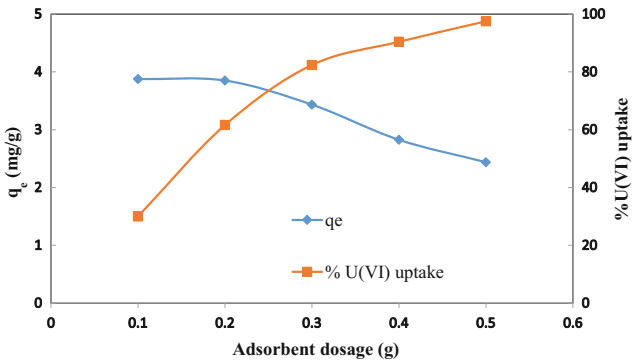

Fig. 10 Effect of adsorbent dosage on the sorption of U(VI) onto silica nanoparticles (initial concentration 50 ppm and 25.0 °C)

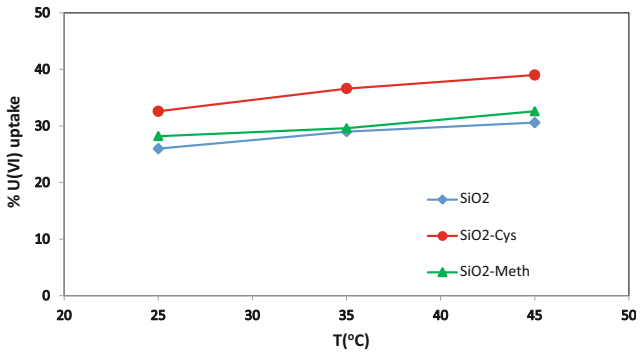

Fig. 11 % Uptake of U(VI) by silica nanoparticles and its modified forms at different temperatures

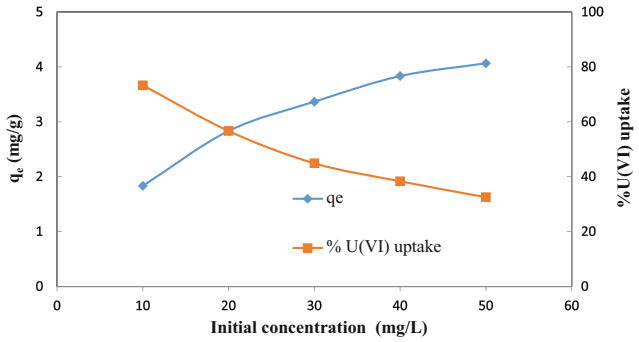

Fig. 12 Effect of initial concentration on the percentage removal and adsorption capacity of U(VI) ions by SiO_2-Cys at pH 3.0 and 25.0 °C

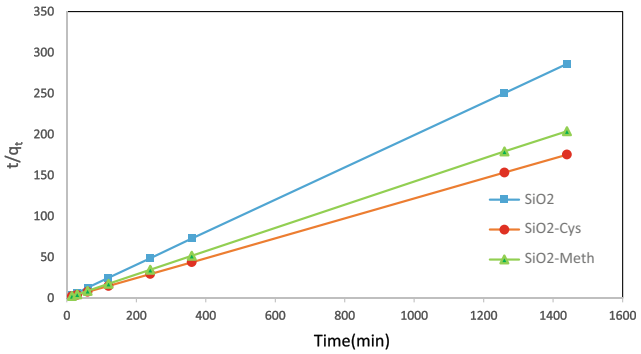

Fig. 14 Pseudo-second order sorption kinetics of uranium (VI) by silica nanoparticles and modified silica nanoparticles at pH 3.0 and 25.0 °C

3.3 Effect of Adsorbent Dose

Figure 10 shows an increase in the percentage uptake of U(VI) with increasing silica nanoparticles dose and reaches 100% uptake at 0.5 g, due to the availability of more binding sites for uranyl ions [52]. Also, it was noticed that 0.1 g of silica nanoparticles has greatest sorption capacity (q_e) for U(VI) ions. Based on economic, environmental and experimental obligations, 0.1 g of silica nanoparticles and its modified forms were used throughout all the experiments.

3.4 Effect of Temperature

Studying the effect of changing temperature (25, 35, 45 °C) on sorption of U(VI) by silica nanoparticles (SiO_2-NPs) and its modified forms, have been done. Figure 11 shows a direct relationship between temperature and percentage uptake of U(VI) ions, which indicated that the sorption mechanism is energy dependent and endothermic [53].

3.5 Effect of Initial Concentration

The effect of initial concentration by silica nanoparticles (SiO_2-NPs) and its modified forms was examined with varying initial U(VI) concentrations (10, 20, 30, 40 and 50 mg/L) with 0.5 g adsorbent dose (Fig. 12). It has been found that increasing concentration of U(VI) solution led to $q_e$increase, and % U(VI) decrease. This can be explained by the availability of surface area and adsorption sites at low initial concentration of U(VI), so it was easily adsorbed and removed. This availability decrease as U(VI) concentration increase, causing a decrease in percentage removal.

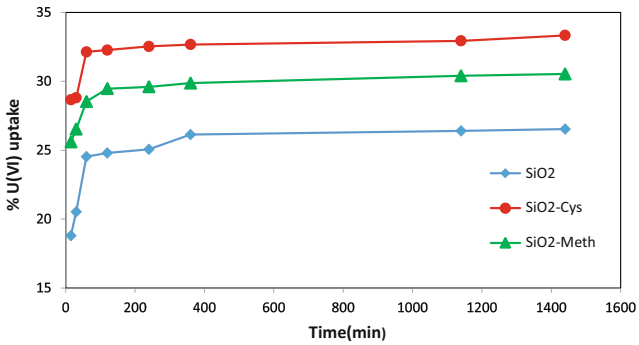

Fig. 13 Uranium (VI) percentage uptake vs. time by unmodified silica nanoparticles and modified silica nanoparticles at pH 3.0 and 25.0 °C

3.6 Effect of Contact Time and Sorption Kinetic Models

Figure 13 shows that the percentage uptake of U(VI) by SiO_2-Cys is higher than that for SiO_2-Meth and for silica nanoparticles (SiO_2-NPs). These results are due to higher percentage loading of cysteine on silica nanoparticles and the binding geometry of cysteine to metal ions (presence of carboxylate group and –SH group). The linear plots of [t/q_t vs. time] were displayed in Fig. 14 for U(VI) sorbed on silica nanoparticles and its modified forms; (SiO_2-Cys) (SiO_2-Meth). Table 5 shows the values of $R^2 = 1$ for pseudo-second-order and the calculated sorption capacity q_e (calculated) was closer to the experimental sorption capacity q_e (experimental), indicating that the pseudo second-order kinetic model describe the sorption process of U(VI) by silica nanoparticles and its modified forms perfectly. Also, that chemisorption process is the rate-controlling step for sorption of U(VI) by silica nanoparticles and its modified forms.

Table 5 Kinetic parameters for sorption of U(VI) by silica nanoparticles and its modified forms at pH 3 and 25 °C

Pseudo-second-order model parameters	SiO_2-NPs	SiO_2-Cys	SiO_2-Meth
k_2 (g/mg.min)	0.035	0.056	0.048
q_e (mg/g) calculated	3.330	4.160	3.830
q_e (mg/g) experimental	3.310	4.166	3.810
R^2	1.000	1.000	1.000

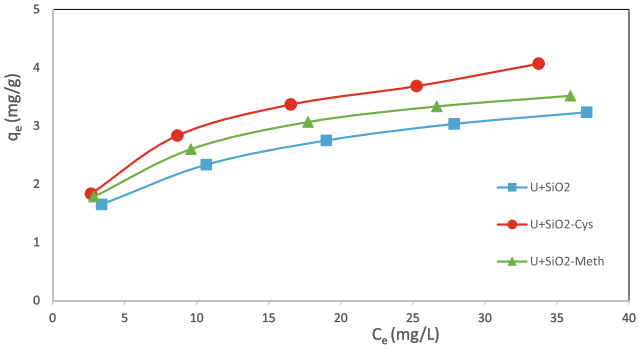

Fig. 15 Plots of adsorption isotherms of U(VI) with silica nanoparticles or its modified forms, at pH 3 and at 25 °C

3.7 Effect of Initial Concentrations and Sorption Isotherm Models

The sorption capacities (q_e) of U(VI) on silica nanoparticles and its modified forms increased with increasing initial concentration of U(VI) at pH 3 (Fig. 15). The reason may be that increasing initial concentration of U(VI) ions provide a significant driving force to overcome the mass transfer resistance between solid phase and aqueous phase, which enhanced the sorption process [54]. The calculated values of isotherm parameters are shown in Table 6 and the sorption of U(VI) on silica nanoparticles shows high correlation coefficients ($R^2 >$ 0.9) for both the Langmuir and Freundlich isotherm model. The possible reason is that both the monolayer and multilayer sorption existed in the sorption process of U(VI) and the presence of homogenous and heterogeneous sites on silica nanoparticles surface, these results agreed with SEM images.

Table 7 Thermodynamic parameters for sorption of U(VI) by silica nanoparticles and its modified forms at 25.0 °C

Metal ion	Adsorbent	ΔG° (kJ/mol)	ΔH° (kJ/mol)	ΔS° (J/mol. K)
U(VI)	SiO_2-NPs	−0.075	9.769	33.033
	SiO_2-Cys	−0.261	3.621	13.028
	SiO_2-Meth	−0.863	3.626	15.065

The values of K_L (Table 6) for sorption of U(VI) by SiO_2-Meth were higher than the other two adsorbents, indicating that the bonding energy of sorption was higher than other two adsorbents [55]. Langmuir isotherm can be used to estimate the value of separation factor (R_L), also called equilibrium parameter. The obtained R_L values were greater than 0 but less than 1 as shown in Table 6, indicating that the sorption processes of U(VI) ion on silica nanoparticles and its modified forms was favorable. In addition, the value of R_L of U(VI) ion on silica nanoparticles and its modified forms lean towards zero (the completely ideal irreversible case) rather than unity (which represents a completely reversible case).

The Freundlich isotherm is the second model used to describe the sorption data of U(VI) and the Freundlich constant K_F ($mg.g^{-1}$) and n are characteristic constants related to the relative sorption capacity of the sorbent and the intensity of sorption, respectively. Table 6 shows that the K_F values for the sorption of U(VI) on silica nanoparticles and its modified forms increased with increasing temperatures, which indicating an endothermic sorption process [56].

Table 6 Langmuir, Freundlich and Dubinin–Radushkevich isotherm parameters for sorption of U(VI) by silica nanoparticles and its modified forms, at different temperatures

T(°C)	Langmuir isotherm				Freundlich isotherm			Dubinin–Radushkevich (D–R)			
	R^2	q_m (mg/g)	K_L (L/mg)	R_L	R^2	nL/mg))	K_F(mg/g)	R^2	β mol^2/kJ^2	q'_m(mg/g)	E kJ/mol))
Silica nanoparticles											
25.0	0.995	3.623	0.193	0.093	0.997	3.521	1.170	0.864	1.430	2.900	0.590
35.0	0.998	3.964	0.222	0.082	0.980	3.484	1.320	0.913	1.173	3.250	0.652
45.0	0.995	4.210	0.221	0.0829	0.995	3.508	1.400	0.869	0.888	3.380	0.750
SiO_2-Cys											
25.0	0.994	4.524	0.206	0.088	0.990	3.246	1.390	0.886	1.102	3.570	0.673
35.0	0.995	5.000	0.210	0.086	0.994	3.125	1.490	0.874	0.869	3.880	0.758
45.0	0.994	5.494	0.215	0.085	0.995	3.030	1.610	0.853	0.663	4.200	0.868
SiO_2-Meth											
25.0	0.997	3.876	0.241	0.076	0.990	3.690	1.370	0.889	1.090	3.190	0.677
35.0	0.995	4.048	0.236	0.078	0.996	3.703	1.425	0.871	0.902	3.290	0.744
45.0	0.994	4.464	0.245	0.075	0.997	3.610	1.550	0.851	0.676	3.580	0.860

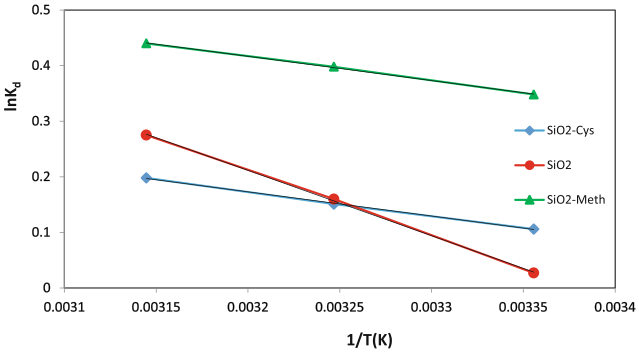

Fig. 16 Plots of $\ln K_d$ vs. 1/T for uranium (VI) on silica nanoparticles and its modified forms

They indicate that SiO_2-Meth has a very high sorption capacity for U(VI) ion than silica nanoparticles and SiO_2-Cys. The values of n were larger than one (Table 6), which indicate that the sorption of U(VI) ion onto silica nanoparticles (SiO_2-NPs) and its modified forms was favorable [57] and for SiO_2-Meth is the most favorable due to the highest value of n. As illustrated in Table 6 the free energy of sorption values (E) calculated from D-R model is less than 8.00 kJ/mol; which insure that physical forces affect the sorption of U(VI) by silica nanoparticles and its modified forms [58].

3.8 Thermodynamics Studies

Thermodynamic functions can be determined using the distribution coefficient, $K_d = q_e/C_e$ which depends on temperature. The change in free energy (ΔG°), enthalpy (ΔH°) and entropy (ΔS°) associated with the adsorption process were calculated by using the following equations:

$$\Delta G^\circ = \Delta H^\circ - T\,\Delta S^\circ \tag{9}$$

Where: R is the universal gas constant (8.314 J/mol K) and T is temperature (K).

$$\ln K_d = \Delta S^\circ/R - \Delta H^\circ/RT \tag{10}$$

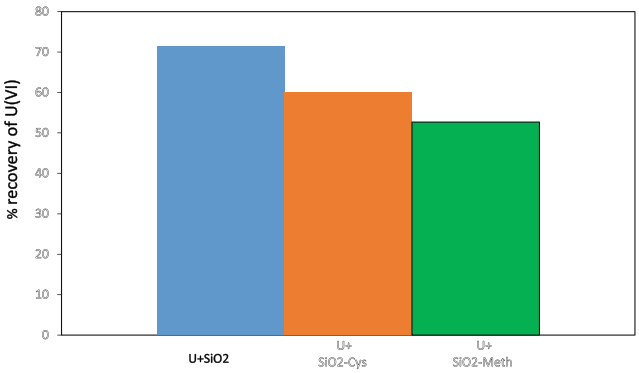

Fig. 17 % recovery for silica nanoparticles and its modified forms using 0.1 M HNO_3

Table 8 Desorption percentage of U(VI) loaded onto silica nanoparticles and its modified forms

	SiO_2-NPs		SiO_2-Cys		SiO_2-Meth	
Conc.[HNO_3]	0.1 M	1.0 M	0.1 M	1.0 M	0.1 M	1.0 M
Recovery stage	% Desorption					
1st 10.0 mL	56.7%	44.7%	49.0%	41.2%	42.9%	38.5%
2nd 10.0 mL	11.6%	9.5%	9.3%	6.9%	7.2%	6.8%
3rd 10.0 mL	3.0%	1.8%	1.6%	1.0%	2.6%	1.5%
%Cumulative recovery	71.3%	56.0%	60.0%	49.1%	52.7%	46.8%

According to the above equation, ΔH° and ΔS° functions can be obtained from the slope and intercept of the plot of $\ln K_d$ versus 1/T yields, respectively as shown in Table 7 and Fig. 16. Results in Table 7 show that SiO_2-Meth has the highest values of Gibbs free energy, which indicated that sorption of uranium (VI) onto SiO_2-Meth is more energetically favorable than silica nanoparticles and SiO_2-Cys and that agreed with K_d values [59]. The positive values of enthalpy change ΔH° (Table 7) indicated that the sorption of uranium (VI) on silica nanoparticles and its modified forms are endothermic process. Also, when the value of ΔH° is less than 40 kJ mol^{-1}, the sorption is a physical process as explained from the value of free energy of sorption (E) in (D-R) isotherm model. Physical sorption is driven by van der Waals and electrostatic forces between the adsorbate and the adsorbent surface. The explanation of the positive values of enthalpy ΔH° is that U(VI) ions are well solvated and in order for the U(VI) ion to be sorbed, they have to lose part of their hydration. This dehydration requires energy and this energy supersedes the exothermicity of the ion getting attached to the surface [58]. The positive values of ΔS° (Table 7) indicate the increased randomness at the solid/solution interface during the sorption process and the affinity of adsorbent for U(VI) ion used. The released surface water molecules, which are displaced by the sorbed species, gain more translational energy than is lost by the adsorbed ions, thus allowing the prevalence of randomness in the system [60].

3.9 Desorption Studies

Desorption processes are important from two points of view: first, the recovery of radionuclide and subsequent use in nuclear energy, secondly the regeneration of sorbent for reuse in other sorption processes. Figure 17 and Table 8 show the percentage cumulative recovery values for silica nanoparticles and its modified forms using two concentrations of nitric acid by cation exchange mechanism. It was found that desorption of uranium(VI) from loaded silica nanoparticles and its modified forms using 0.1 M HNO_3 is more efficient than 1.0 M HNO_3 [61] with more desorption percentage for uranium(VI)

with 71.3% from silica nanoparticles than modified forms. The lowest value of cumulative recovery percentage for SiO_2-Meth than SiO_2-NPs and SiO_2-Cys explain its greatest tendency in holding U(VI), and these results agreed with higher value of K_d for SiO_2-Meth. SiO_2-Meth could be used in removal of metal ions from solution and concentrating them to be removed as solid radioactive waste.

4 Conclusions

Silica nanoparticles and its modified forms with cysteine or methionine amino acids are able to be used as efficient adsorbents for removal-separation of U(VI) ions from aqueous solutions. Modified silica nanoparticles with cysteine (SiO_2-Cys) ~33% or methionine (SiO_2-Meth) ~30% improve the uptake of uranium ions with respect to unmodified silica nanoparticles ~27%. The experimental adsorption data was well described by the pseudo second-order kinetic model. Thermodynamic studies of the processes show that the adsorption is spontaneous with positive enthalpy and entropy changes. The highest percent recovery for U(VI) using 0.1 M HNO_3 was achieved from silica nanoparticles (~ 71%) than its modified forms SiO_2-Cys and SiO_2-Meth.

References

1. Ali O, Osman H, Sayed S, Shalabi M (2015) The removal of uranium and thorium from their aqueous solutions via glauconite. Desalin Water Treat 53:760–767
2. Majdan M, Pikus S, Gajowiak A, Sternik D, Zieba E (2010) Uranium sorption on bentonite modified by octadecyltrimethylammonium bromide. J Hazard Mater 184:662–670
3. Dolatyari H, Yaftian M, Rostamnia S (2016) Removal of uranium(VI) ions from aqueous solutions using Schiff base functionalized SBA-15 mesoporous silica materials. J Environ Manag 169:8–17
4. Talip Z, Eral M, Hicsonmez U (2009) Sorption of thorium from aqueous solutions by perlite. J Environ Radioact 100:139–143
5. Simsek S, Baybas D, Koçyigit MC, Yıldırım H (2014) Organoclay modified with lignin as a new adsorbent for removal of Pb^{2+} and UO_2^{2+}. J Radioanal Nucl Chem 299:283–292
6. Guo Z, Yu X, Guo F, Tao Z (2005) Th(IV) sorption on alumina: effects of contact time, pH, ionic strength and phosphate. J Colloid Interface Sci 288:14–20
7. Kutahyali C, Eral M (2004) Selective sorption of uranium from aqueous solutions using activated carbon prepared from charcoal by chemical activation. Sep Purif Technol 40(2):109–114
8. Khalili F, Salameh N, Shaybe M (2013) Sorption of uranium(VI) and thorium(IV) by Jordanian Bentonite. J Chem:1–10
9. Khalili F, Al-Shaybe M (2009) Sorption of thorium (IV) and uranium (VI) by Tulul al-Shabba Zeolitic Tuff, Jordan. J Earth Environ Sci 2:108–119
10. Sadeghi S, Azhdari H, Arabi H, Oghaddam AZ (2012) Surface modified magnetic Fe_3O_4 nanoparticles as a selective sorbent for solid phase extraction of uranyl ions from water samples. J Hazard Mater 215:208–216
11. Crini G, Lichtfouse E, Wilson L, Crini N (2018) Green adsorbents for pollutant removal, Environmental chemistry for a sustainable world 18. Cham Springer, 23–71
12. Barik TK, Sahu B, Swain V (2008) Silica nanoparticles-from medicine to pest control. Parasitol Res 103:253–258
13. Subbiah R, Veerapandian M, Yun KS (2010) Nanoparticles: functionalization and multifunctional applications in biomedical sciences. Curr Med Chem 17:4559–4577
14. Mathe C, Devineau S, Aude J, Lagniel G, Chedin C, Legros V, Mathon M (2013) Structural determinants for protein sorption/nonsorption to silica surface. PLoS One 8(11):81346
15. Townsend DM, Tew KD, Tapiero H (2004) Sulfur containing amino acids and human disease. Biomed Pharmacother 58(1):47–55
16. Conte ML, Jakob U, Reichmann D (2013) Oxidative stress and redox regulation. Chapter one, Springer New York
17. Lambert JF (2008) Sorption and polymerization of amino acids on mineral surfaces: a review. Orig Life Evol Biosph 38:211–242
18. Ashley CE, Carnes EC, Phillips GK, Padilla D, Durfee PN, Brown PA, Hanna TN, Liu J, Phillips B, Carter MB (2011) The targeted delivery of multicomponent cargos to cancer cells by nanoporous particle-supported lipid bilayers. Nat Mater 10:389–397
19. Tarn D, Ashley CE, Xue M, Carnes EC, Zink JI, Brinker CJ (2013) Mesoporous silica nanoparticle nanocarriers: biofunctionality and biocompatibility. Acc Chem Res 46:792–801
20. Patwardhan SV, Emami FS, Berry RJ, Jones SE, Naik RR, Deschaume O, Heinz H, Perry CC (2012) Chemistry of aqueous silica nanoparticle surfaces and the mechanism of selective peptide sorption. J Am Chem Soc 134:6244–6256
21. Grzegorczyk DS, Carta G (1996) Sorption of amino acids on porous polymeric adsorbents—II. Intraparticle mass transfer. Chem Eng Sci 51(5):819–826
22. Ikahsan J, Johnson BB, Wells JD, Angove MJ (2004) Sorption of aspartic acid on kaolinite. J Colloid Interface Sci 273(1):1–5
23. Vinu A, Hossain KZ, Kumar GS, Ariga K (2006) Sorption of L-histidine over mesoporous carbon molecular sieves. Carbon 44:530
24. Krohn JE, Tsapatsis M (2005) Amino acid sorption on zeolite beta. Langmuir 21(9):8743–8750
25. Faghihian H, Nejati-Yazdinejad M (2009) Equilibrium study of sorption of L-cysteine by natural bentonite. Clay Miner 44:125–133
26. Nam NS, Khang DN, Tuan LQ, Son LT (2016) Surface modification of silica nanoparticles by hexamethyldisilazane and n-butanol. Int J Env Tech Sci 2:31–37
27. Doi E, Shibata D, Matoba T (1981) Modified calorimetric ninhydrin methods for peptidase assay. Anal Biochem 118:173–184
28. Orabi AH (2013) Determination of uranium after separation using solvent extraction from slightly nitric acid solution and spectrophotometric detection. J Radiat Res Appl Sci 6:1–10
29. Azizian S (2004) Kinetic models of sorption: a theoretical analysis. J Colloid Interface Sci 276:47–52
30. Langmuir I (1918) The sorption of gases on plane surfaces of glass, mica and platinum. J Am Chem Soc 40:1361–1403
31. Freundlich H (1906) Over the sorption in solution. J Phys Chem 57: 385–470
32. Dubinin MM, Radushkevich LV (1947) Equation of the characteristic curve of activated charcoal. Chemisches Zentralblatt 1:875
33. Fan F, Pan D, Wu H, Zhang H, Wu W (2017) Succinamic acid grafted nano silica for the preconcentration of U(VI) from aqueous solution. Ind Eng Chem Res 56(8):2221–2228
34. Khataee A, Movafeghi A, Nazari F, Vafaei F, Dadpour M, Hanifehpour Y, Joo S (2014) The toxic effects of L-cysteine-capped cadmium sulfide nanoparticles on the aquatic plant Spirodela polyrrhiza. J Nanopart Res 16:2774–2784
35. Parker SF (2013) Assignment of the vibrational spectrum of L-cysteine. Chem Phys 424:75–79

36. Wolpert M, Hellwig P (2006) Infrared spectra and molar absorption coefficients of the 20 alpha amino acids in aqueous solutions in the spectral range from 1800 to 500 cm^{-1}. Spectrochim Acta A 64:987–1001
37. Jafari V, Allahverdi A (2014) Synthesis and characterization of colloidal silica nanoparticles via an ultrasound assisted route based on alkali leaching of silica fume. Int J Nanosci Nanotechnol 10(3): 145–152
38. Chen H, Bian H, Li J, Guo X, Wen X, Zheng J (2013) Molecular conformations of crystalline L-cysteine determined with vibrational cross angle measurements. J Phys Chem B 117:15614–15624
39. Hautala J, Airaksinen S, Naukkarinen N, Vainio O, Juppo A (2014) Evaluation of new flavors for feline mini-tablet formulations. J Excip Food Chem 5(2):80–100
40. Sompech S, Dasri T, Thaomola S (2016) Preparation and characterization of amorphous silica and calcium oxide from agricultural wastes. Orient J Chem 32(4):1923–1928
41. Fuad A, Mufti N, Diantoro M, Septa KS (2016) Synthesis and characterization of highly purified silica nanoparticles from pyrophyllite ores. In: AIP conference proceedings, 1719, 030020-5
42. Dakova I, Vasileva P, Karadjova I (2011) Cysteine modified silica submicrospheres as a new sorbent for preconcentration of Cd (II) and Pb (II). Bulg Chem Commun 43(2):210–216
43. Sing K, Everett DH, Haul RAW, Moscou L, Pierotti RA, Rouquerol J, Siemieniewska T (1985) Reporting physisorption data for gas/solid systems with special reference to the determination of surface area and porosity. Pure App Chem 57(4):603–619
44. Chaves M, Valsaraj K, DeLaune R, Gambrell R, Buchler P (2011) Mercury uptake by biogenic silica modified with L-cysteine. Environ Technol 32(14):1615–1625
45. Khantana N, Shadjoua N, Hasanzadeh M (2019) Synthesize of dendritic fibrous nano-silica functionalized by cysteine and its application as advanced adsorbent. Nanocomposites 5(4):104–113
46. Kim K, Kim H, Lee W, Lee C, Kim T, Lee J, Jeong J, Paek S, Oh J (2014) Surface treatment of silica nanoparticles for stable and charge-controlled colloidal silica. Int J Nanomedicine 9:29–40
47. Du M, Zheng Y (2007) Modification of silica nanoparticles and their application in UDMA dental polymeric composites. Polym Compos 28(2):198–207
48. Wu J, Ma G, Li P, Ling L, Wang B (2014) Surface modification of silica nanoparticles with acrylsilane-containing tertiary amine structure and their effect on the properties of UV-curable coating. J Coat Technol Res 11(3):387–395
49. Weiss IM, Muth C, Drumm R, Kirchner H (2018) Thermal decomposition of the amino acids glycine, cysteine, aspartic acid, asparagine, glutamic acid, glutamine, arginine and histidine. BMC Biophys 11(1):1–15
50. Belachew N, Devi R, Basavaiah K (2016) Facile green synthesis of L-methionine capped magnetite nanoparticles for sorption of pollutant Rhodamine B. J Mol Liq 224:713–720
51. Wang R, Wei Y, Jiang H, Gong H (2018) Sorption of uranium(VI) on mesoporous silica microspheres supported titanium hydroxide hybrid material. J Radioanal Nucl Chem 318(3):2023–2032
52. Fan T, Liu Y, Feng B, Zeng G, Yang C, Zhou M, Zhou H, Wang X (2008) Biosorption of cadmium(II), zinc(II) and lead(II) by Penicillium simplicissimum: isotherms, kinetics and thermodynamics. J Hazard Mater 160(2–3):655–661
53. Huang Y, Hu Y, Chen L, Yang T, Huang H, Shi R, Lu P, Zhong C (2018) Selective biosorption of thorium (IV) from aqueous solutions by ginkgo leaf. PLoS One 13(3):0193659
54. Naseem Z, Bhatti H, Sadaf S, Noreen S, Ilyas S (2016) Sorption of uranium (VI) by Trapa bispinosa from aqueous solution, effect of pretreatments and modeling studies. Desalin Water Treat 57(24): 11121–11132
55. Ebrahimi-Gatkash M, Younesi HN, Heidari A (2015) Amino-functionalized mesoporous MCM-41 silica as an efficient adsorbent for water treatment: batch and fixed-bed column sorption of the nitrate anion. Appl Water Sci 7(4):1887–1901
56. Kaynar UH, Ayvacıklı M, Hiçsönmez U, Kaynar SC (2015) Removal of thorium (IV) ions from aqueous solution by a novel nanoporous ZnO: isotherms, kinetic and thermodynamic studies. J Environ Radioact 150:145–151
57. Chegrouche S, Mellah A, Barkat M, Aknoun A (2016) Kinetics and isotherms for uranium (VI) sorption from aqueous solutions by goethite. Am J Chem Mater Sci 3(2):6–12
58. Donat R, Akdogan A, Erdem E, Cetisli H (2005) Thermodynamics of Pb^{2+} and Ni^{2+} sorption onto natural bentonite from aqueous solutions. J Colloid Interface Sci 286(1):43–52
59. Xia L, Tan K, Wang X, Zheng W, Liu W, Deng C (2013) Uranium removal from aqueous solution by banyan leaves: equilibrium, thermodynamic, kinetic, and mechanism studies. J Environ Eng 139: 887–895
60. Khalili F, Al-Banna G (2015) Sorption of uranium(VI) and thorium(IV) by insolubilized humic acid from Ajloun soil – Jordan. J Environ Radioact 146:16–26
61. Liu C, Liang X, Liu J, Yuan W (2016) Desorption of copper ions from the polyamine functionalized adsorbents: behaviors and mechanisms. Sorpt Sci Technol 34(7–8):455–468